

Prediction Accuracy of Artificial Neural Networks in Thermal Management Applications Subject to Neural Network Architectures

Mohammad Reza Shaeri¹, Andoniaina M. Randriambololona¹, Soroush Sarabi²

¹Department of Mechanical Engineering, University of the District of Columbia, Washington, DC 20008, USA
mohammadreza.shaeri@udc.edu; andoniainam.randriam@udc.edu

²Raderon AI Lab, Burnaby, BC, Canada
s.sarabi@raderonlab.ca

Abstract - The present study investigates the dependency of prediction accuracy of an artificial neural network (ANN) on the network architecture using 65 different neural networks from seven architecture patterns. The accuracy of the ANNs is compared based on their capability to predict heat transfer coefficients of air-cooled heat sinks operating in laminar flow. Scattered input data is used for training the networks to make the modelling more realistic and closer to practical applications. The input variables for the neural network are heat sink width, channel height, channel length, number of channels, fin thickness, and Reynolds number. The output is heat transfer coefficient. The training process for all ANNs is performed using ReLU as the activation function. The accuracy of the neural networks is evaluated by the root mean square error. It is found that the prediction accuracy of an ANN is strongly dictated by the optimization of the network architecture, which corresponds to the proper number of hidden layers and the number of neurons at each layer. The most accurate architecture in the present study predicts heat transfer coefficients of 60% and 86% of heat sinks within $\pm 10\%$ and $\pm 20\%$ of the true values, respectively. However, an ANN with an unoptimized architecture results in a substantially reduced accuracy such that it predicts heat transfer coefficients of only 19% and 30% of heat sinks within $\pm 10\%$ and $\pm 20\%$ of the true values, respectively.

Keywords: Artificial neural network; Network architecture; Prediction accuracy; Scattered data; Heat sink; Heat transfer coefficient.

1. Introduction

An artificial neural network (ANN), a subset of machine learning, is a data processing system that mimics the characteristics of the human brain to predict the performances of engineering systems [1, 2]. The feed-forward multilayer perceptron ANN model consists of interconnected nodes, called neurons, which form an input layer, hidden layer(s), and an output layer [3, 4]. Inputs are received in the input layer, and outputs are generated in the output layer. The information from the input layer to the output layer is transformed via the intermediate hidden layer(s). Fig. 1 illustrates an ANN with five neurons in the input layer, three hidden layers with 16, 10, and 12 neurons in the first, second, and third hidden layers, respectively, and one output in the output layer. Each neuron is associated with weights and a bias. The outputs of all the neurons in one layer act as the inputs for the neurons in the next layer. The feed-forward implies that the inputs always propagate forward through the network [5]. Preparation of the input dataset, which is obtained through experiments, simulations, etc., is a crucial step of an ANN model. The input dataset is randomly divided into three parts: training, validation, and testing. The neural network learns the input-output patterns from the training dataset, the trained performance is assessed using the validation dataset, and finally the accuracy of the network is evaluated using the testing dataset [6]. The output transferred from the k th neuron of the $(n - 1)$ th layer to the j th neuron of the n th layer is described as follows [7]:

$$x_j^n = f_n \left(\sum_k w_{jk}^n x_k^{n-1} + b_j^n \right) \quad (1)$$

where x_j^n is the output, f_n is the activation function of layer n , b_j^n is the bias of the j th neuron in the n th layer, and w_{jk}^n is the weight from the k th neuron of the $(n - 1)$ th layer to the j th neuron of the n th layer. The loss function (E) corresponds

to the magnitude of the error between the predicted values and true values. In this study, the loss function is defined as the root mean square error (RMSE), as follows [8]:

$$E = \sqrt{\frac{1}{n} \sum_{i=1}^n (\hat{y}_i - y_i)^2} \quad (2)$$

where \hat{y}_i and y_i are the i th predicted output and the true value, respectively. Then, through an iterative process, the weights and biases are updated using gradient descent algorithms, as shown below:

$$w_k = w_k - \eta \frac{\partial E}{\partial w_k} \quad (3)$$

$$b_j = b_j - \eta \frac{\partial E}{\partial b_j} \quad (4)$$

where η is the learning rate. When the training process is complete, the accuracy of the network is evaluated using the testing dataset. In this study, the accuracy of the neural network to predict the outputs is also evaluated by RMSE.

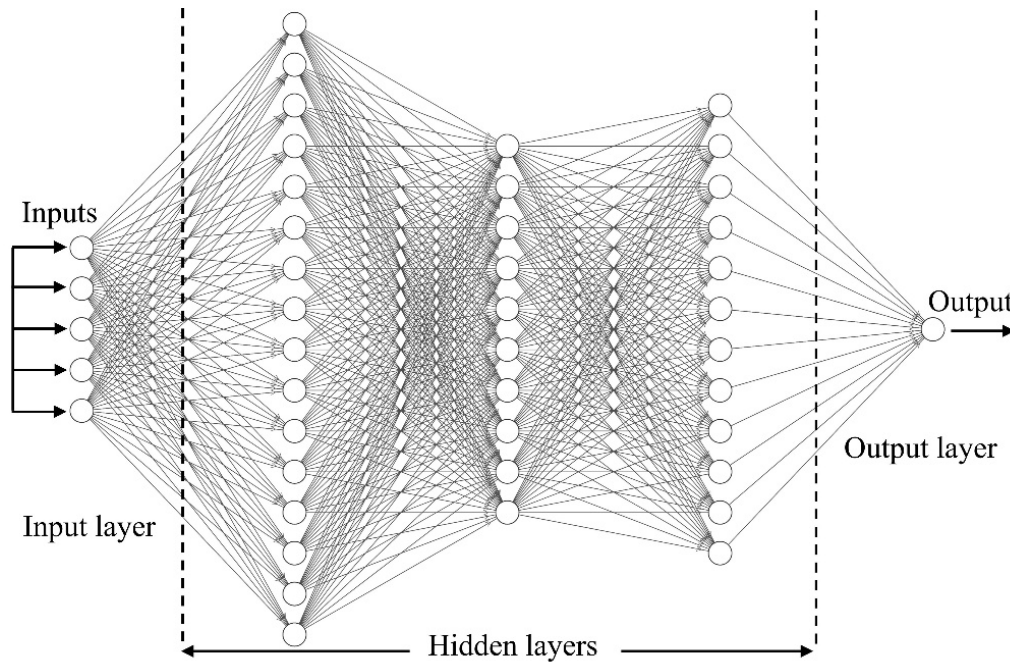


Fig. 1: Architecture of an artificial neural network with three hidden layers.

2. Motivation and Problem Description

One of the unique advantages of ANNs is their capability to develop correlations through datasets [9]. The data can be a set of scattered experimental data acquired under various operating and design conditions and documented as a bank of datasets in literature. Unlike regular input datasets that follow specified relations, there are no relations among the scattered data. Such limitation results in challenges for interpolation techniques to develop correlations through

scattered data [10]. Apart from this, there may be a lack of sufficiently large numbers of data that exist in literature; as a result, developing correlations through a low number of scattered datasets is even more challenging and requires more effective techniques such as ANNs. The prediction accuracy of an ANN strongly depends on optimizing the architecture of the neural network, which corresponds to obtaining an appropriate number of hidden layers and neurons at each layer. However, the optimization of a network architecture is usually performed through the trial-and-error technique [11]. The motivation of the present study is to evaluate the effect of the neural network architecture on the prediction accuracy of an ANN. For this purpose, the accuracy of ANNs with different network architectures is assessed and compared by the prediction of the heat transfer coefficient (h) in air-cooled heat sinks. Air-cooled heat sinks consist of a series of parallel rectangular cross-sectional channels separated by fins and are widely used for thermal management in broad applications due to their simplicity and low-cost manufacturing process [12]. Fig. 2 illustrates a schematic of a heat sink, in which H , L , and W_{ch} are the channel height, length, and width, respectively, W is the width of the heat sink, t_f is the fin thickness, and t_b is the thickness of the base of the heat sink.

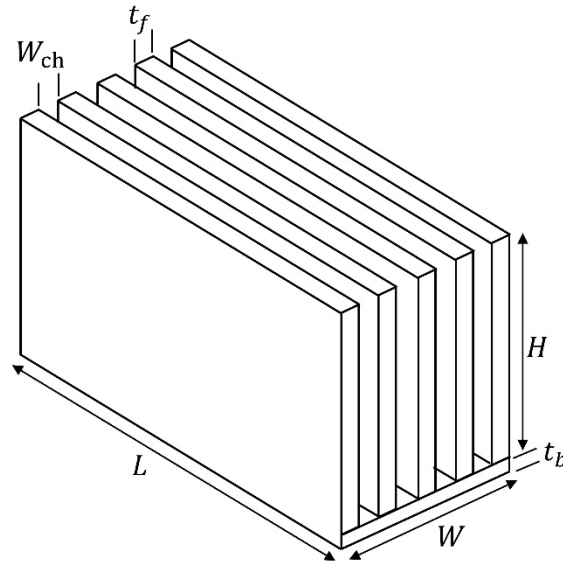


Fig. 2: Schematic of a parallel plate-finned heat sink.

In the present study, the input dataset is prepared using the correlations developed by Teertstra et al. [13] to predict h in high aspect ratio parallel plate-finned heat sinks operating in laminar flow. The correlations consider the effects of both fully developed and developing flow between parallel plates, as follows:

$$h = \frac{\tanh \sqrt{2Nu_i \frac{k_f H^2}{k_s W_{ch} t_f} \left(\frac{t_f}{L} + 1 \right)}}{\sqrt{2Nu_i \frac{k_f H^2}{k_s W_{ch} t_f} \left(\frac{t_f}{L} + 1 \right)}} Nu_i \frac{k_f}{W_{ch}} \quad (5)$$

$$Nu_i = \left[\frac{1}{\left(\frac{Re_b^* Pr}{2}\right)^3} + \frac{1}{\left(0.664 \sqrt{Re_b^*} Pr^{1/3} \sqrt{1 + \frac{3.65}{\sqrt{Re_b^*}}}\right)^3} \right]^{-1/3} \quad (6)$$

$$Re_b^* = \frac{\rho U W_{ch}}{\mu} \times \frac{W_{ch}}{L} \quad (7)$$

where Nu_i is the ideal Nusselt number, Pr , k_f , ρ , μ , and U are air Prandtl number, thermal conductivity, density, viscosity, and average velocity in channel, respectively, and k_s is the thermal conductivity of the solid (i.e., aluminium in this paper). In the present study, 65 different neural network architectures categorized in seven patterns are considered, and their accuracy for the prediction of h is compared. The different architecture categories are a result of the pattern of the hidden layers and neurons inside the hidden layers and consist of (1) single-layer pattern (SLP), which corresponds to only a single hidden layer; (2) linear pattern (LP), which corresponds to multiple hidden layers in a series with one neuron at each layer; (3) rectangular pattern (RP), which corresponds to multiple hidden layers in a series with the same number of neurons at each layer; (4) square pattern (SP), which is a special case of rectangular pattern in which the number of neurons at each layer is equal to the total number of hidden layers; (5) backward triangular pattern (BTP) in which the number of hidden layers and the number of neurons at each layer form a network configuration like a backward triangle; (6) forward triangular pattern (FTP), which is similar to the BTP but with forward configuration; and (7) rhombus pattern (RHP), in which the number of hidden layers and the number of neurons at each layer form a rhombus. Tables 1 and 2 list the information about all neural networks in this paper. In these tables, ANN, N_{HL} , N_N , and N_t stand for the ANN's number (i.e., ID), number of hidden layers in the architecture, number of neurons at each hidden layer, and total number of neurons in the network, respectively.

Table 1: Information of the neural network architectures of SLP, LP, RP, and SP.

Single-layer pattern (SLP)				Linear pattern (LP)				Rectangular pattern (RP)				Square pattern (SP)			
ANN	N_{HL}	N_N	N_t	ANN	N_{HL}	N_N	N_t	ANN	N_{HL}	N_N	N_t	ANN	N_{HL}	N_N	N_t
1	1	2	2	16	2	1	2	25	2	2	4	37	8	8	64
2	1	4	4	17	4	1	4	26	4	4	16	38	16	16	256
3	1	8	8	18	8	1	8	27	6	8	48	39	32	32	1024
4	1	16	16	19	16	1	16	28	8	16	128	40	64	64	4096
5	1	32	32	20	32	1	32	29	10	32	320	41	128	128	16384
6	1	64	64	21	64	1	64	30	12	64	768	42	256	256	65536
7	1	128	128	22	128	1	128	31	14	128	1792				
8	1	256	256	23	256	1	256	32	16	256	4096				
9	1	512	512	24	512	1	512	33	18	512	9216				
10	1	1024	1024					34	20	1024	20480				
11	1	2048	2048					35	22	2048	45056				
12	1	4096	4096					36	24	4096	98304				
13	1	8192	8192												
14	1	16384	16384												
15	1	32768	32768												

Table 2: Information of the neural network architectures of BTP, FTP, and RHP.

Backward triangular pattern (BTP)				Forward triangular pattern (FTP)				Rhombus pattern (RHP)			
ANN	N_{HL}	N_N	N_t	ANN	N_{HL}	N_N	N_t	ANN	N_{HL}	N_N	N_t
43	2	2...1	3	51	2	1...2	3	59	3	1...2...1	4
44	4	4...1	10	52	4	1...4	10	60	7	1...4...1	16
45	8	8...1	36	53	8	1...8	36	61	15	1...8...1	64
46	16	16...1	136	54	16	1...16	136	62	31	1...16...1	256
47	32	32...1	528	55	32	1...32	528	63	63	1...32...1	1024
48	64	64...1	2080	56	64	1...64	2080	64	127	1...64...1	4096
49	128	128...1	8256	57	128	1...128	8256	65	255	1...128...1	16384
50	256	256...1	32896	58	256	1...256	32896				

For all the ANNs, the input layer includes six neurons/inputs which are W , H , L , N , t_f , and Re (Reynolds number, calculated based on the hydraulic diameter of the channel). The output layer includes only one output, which is heat transfer coefficient. To make the problem close to the practical applications, it is assumed that there is only a limited available number of scattered datasets. Therefore, 200 scattered datapoints are selected from the following ranges: $5 \text{ cm} \leq W \leq 60 \text{ cm}$, $5 \text{ cm} \leq L \leq 80 \text{ cm}$, $1 \text{ cm} \leq H \leq 5 \text{ cm}$, $0.6 \text{ mm} \leq t_f \leq 1 \text{ mm}$, $6 \leq H/W_{ch} \leq 15$, and $400 \leq Re \leq 2200$. Also, t_b does not have any impact on the calculation of h using Eqs. (5) to (7). Among 200 input data, 35% and 15% are chosen randomly for the training and validation, respectively. The remaining 50% is used for testing. The backpropagation algorithm is implemented for the training process. Also, $\eta = 0.001$, and ReLU is the activation function due to its effectiveness. Adam optimizer is used to improve training speed and accuracy for updating the weights and biases [14].

3. Results

All the trainings were performed for over 1000 epochs. The training process was converged when negligible changes in RMSE were obtained beyond a threshold epoch number. Then, the testing dataset was used for evaluating the accuracy of the neural networks to predict h . Since an input dataset may have a wide range of values, it may reduce the accuracy of the ANN. To improve the prediction accuracy, the input dataset is normalized to be ranged between 0 and 1 [15]. Fig. 3 illustrates the RMSE of individual neural networks corresponding to the normalized input dataset.

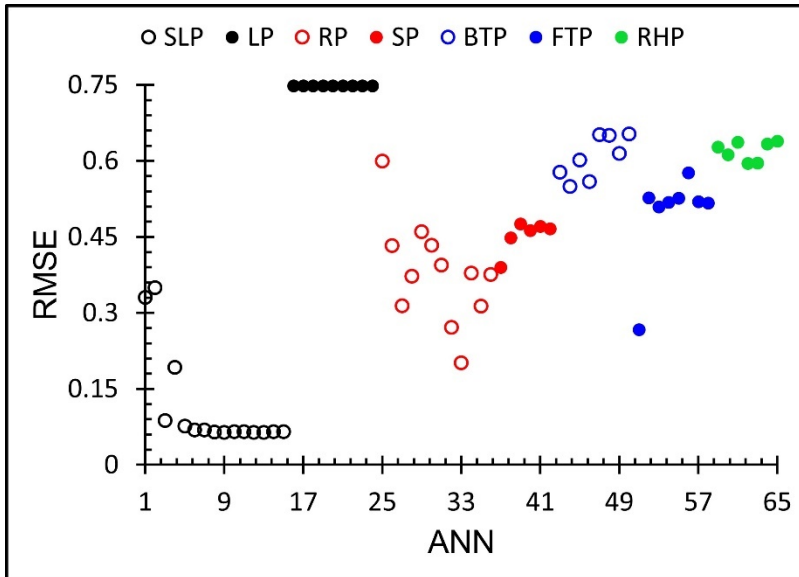


Fig. 3: RMSE for ANNs investigated in this study.

Among seven categories of neural networks, the SLP and LP results in the highest and lowest accuracy, respectively. Among all neural networks, ANN 13 leads to the highest accuracy (i.e., the network with the lowest RMSE).

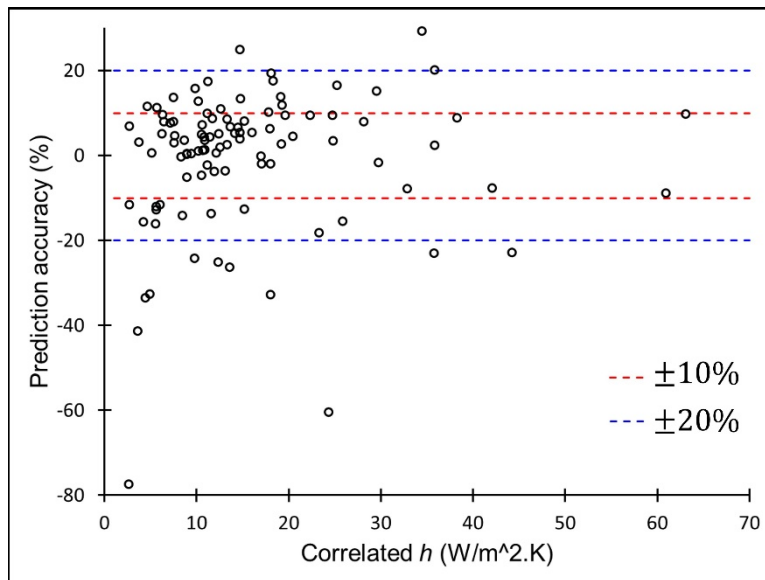


Fig. 4: Prediction accuracy of ANN 13 with the lowest RMSE.

Since the most accurate ANN has been identified, it can be used as a design tool to predict h in air-cooled heat sinks. To evaluate the performance of ANN 13, its accuracy for predicting h in 100 new heat sinks with a wide range of h values is assessed and illustrated in Fig. 4. These 100 new heat sinks have not been observed by the ANNs before.

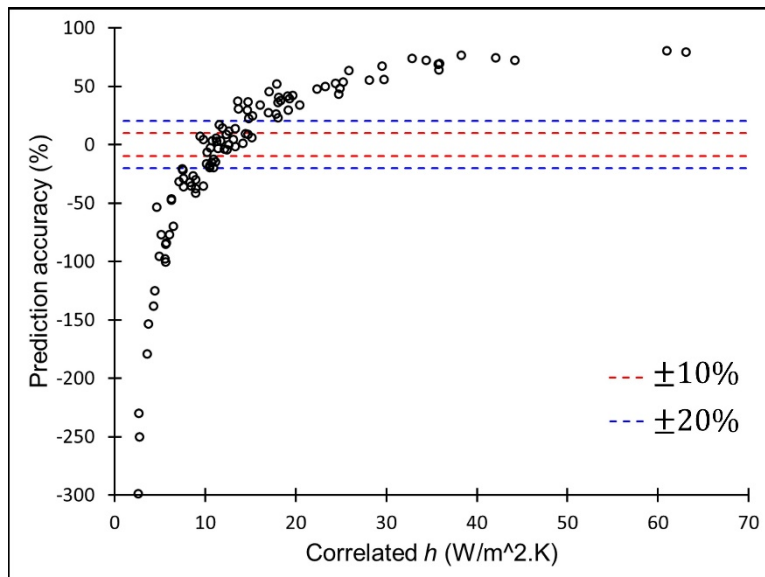


Fig. 5: Prediction accuracy of ANN 61 with a high RMSE.

To gain a better understanding of the impact of the optimized network architecture on the prediction accuracy, the same 100 heat sinks are used to assess the accuracy of ANN 61 as one of the ANNs with a high RMSE, as illustrated in

Fig. 5. The difference between the predicted and true values is calculated as $(h_t - h_p)/h_t \times 100$, which h_t and h_p stand for the true h that is obtained from the correlations, and predicted h by the ANN, respectively. Based on Fig. 4, the ANN 13 predicts h with excellent accuracy given that the heat transfer coefficients of 60% and 86% of heat sinks are predicted within $\pm 10\%$ and $\pm 20\%$ of true values, respectively. However, based on Fig. 5, ANN 61 results in a poor prediction such that only 19% and 30% of heat transfer coefficients are predicted within $\pm 10\%$ and $\pm 20\%$ of true values, respectively. These findings indicate the crucial role of an optimized neural architecture on the prediction accuracy of ANNs as potential design tools in thermal management applications.

4. Conclusion

The important role of the optimized architecture of a neural network on the prediction accuracy of the ANN was demonstrated by comparing the performances of 65 ANNs that predict heat transfer coefficients of air-cooled heat sinks. The scattered input dataset was used for the training and testing processes to make the problem close to practical applications. While the network with an optimized architecture predicted heat transfer coefficient of 86% of heat sinks within $\pm 20\%$ of the true values, poor predictions were obtained by an ANN with an unoptimized architecture as the heat transfer coefficients of only 30% of heat sinks were predicted within $\pm 20\%$ of the true values.

Acknowledgements

This research is supported by the National Science Foundation-CREST Award (Contract #HRD-1914751) and the Department of Energy/National Nuclear Security Agency (DE-FOA-0003945).

References

- [1] F. Jalilantabar, R. Mamat, S. Kumarasamy, "Prediction of lithium-ion battery temperature in different operating conditions equipped with passive battery thermal management system by artificial neural networks," *Mater. Today: Proc.*, vol. 48, pp. 1796-1804, 2022.
- [2] S. Tian, N. I. Arshad, D. Toghraie, S. A. Eftekhari, M. Hekmatifar, "Using perceptron feed-forward Artificial Neural Network (ANN) for predicting the thermal conductivity of graphene oxide- Al_2O_3 /water-ethylene glycol hybrid nanofluid," *Case Stud. Therm. Eng.*, vol. 26, p. 101055, 2021.
- [3] C. M. Salgado, R. S. F. Dam, E. J. A. Puertas, W. L. Salgado, "Calculation of volume fractions regardless scale deposition in the oil industry pipelines using feed-forward multilayer perceptron artificial neural network and MCNP6 code," *Appl. Radiat. Isot.*, vol. 185, p. 110215, 2022.
- [4] B. N. Mengesha, M. R. Shaeri, S. Sarabi, "Artificial neural network to predict pressure drops in heat sinks," in *Proceedings of the 9th International Conference on Fluid Flow, Heat and Mass Transfer (FFHMT'22)*, Niagara Falls, Canada, 2022.
- [5] K. C. Santosh, N. Das, S. Ghosh, "Chapter 2 - Deep learning: a review," in *Deep Learning Models for Medical Imaging*, KC Santosh, Nibaran Das, Swarnendu Ghosh, Ed. Academic Press, 2022, pp. 29-63.
- [6] X. Cheng, F. Ren, Z. Gao, L. Zhu, Z. Huang, "Synergistic effect analysis on sooting tendency based on soot-specialized artificial neural network algorithm with experimental and numerical validation," *Fuel*, vol. 315, p. 122538, 2022.
- [7] J. Moon, D. Q. Gbadago, G. Hwang, D. Lee, S. Hwang, "Software platform for high-fidelity-data-based artificial neural network modeling and process optimization in chemical engineering," *Comput. Chem. Eng.*, vol. 158, p. 107637, 2022.
- [8] J. C. Nsangou, J. Kenfack, U. Nzotcha, P. S. N. Ekam, J. Voufo, T. T. Tamo, "Explaining household electricity consumption using quantile regression, decision tree and artificial neural network," *Energy*, vol. 250, p. 123856, 2022.
- [9] W. J. Lee, K. J. Bae, O. K. Kwon, "Development of heat transfer correlation for falling film absorber using artificial neural network model," *Int. J. Heat Mass Transfer*, vol. 183, p. 122209, 2022.
- [10] Z. Chen, F. Cao, "Scattered data approximation by neural networks operators," *Neurocomputing*, vol. 190, pp. 237-242, 2016.

- [11] J. O. B. Lira, H. G. Riella, N. Padoin, C. Soares, “Computational fluid dynamics (CFD), artificial neural network (ANN) and genetic algorithm (GA) as a hybrid method for the analysis and optimization of micro-photocatalytic reactors: NO_x abatement as a case study,” *Chem. Eng. J.*, vol. 431, p. 133771, 2022.
- [12] M. R. Shaeri, R. Bonner, H. Pearlman, “Enhancing heat transfer rates across different flow regimes using perforated-finned heat sinks,” in *Proceedings of the Second Thermal and Fluids Engineering Conference, ASTFE Digital Library. Begel House Inc.*, Las Vegas, NV, 2017, pp. 1219-1228.
- [13] P. Teertstra, M. M. Yovanovich, J. R. Culham, “Analytical forced convection modeling of plate fin heat sinks,” *J. Electronics Manufacturing*, vol. 10, pp. 253-261, 2000.
- [14] A. Poro, S. Sarabi, S. Zamanpour, S. Fotouhi, F. Davoudi, S. Khakpash, S. Ranjbar Salehian, T. Madayen, A. Foroutanfar, E. Bakhshi, N. S. Mahdavi, F. Alicavus, A. Mazidabadi Farahani, G. Sabbaghian, R. S. Hosseini, A. Aryaeefar, M. Hemati, “Investigation of the orbital period and mass relations for W UMA-type contact systems,” *MNRAS*, vol. 510, pp. 5315-5329, 2022.
- [15] M. Mohseni, F. Aghazadeh, N. Arjmand, “Improved artificial neural networks for 3D body posture and lumbosacral moment predictions during manual material handling activities,” *J. Biomech.*, vol. 131, p. 110921, 2022.